ACS OMEGA

Article

Cite This: ACS Omega 2018, 3, 10255−10266

http://pubs.acs.org/journal/acsodf

Activity of Co^{II}−Quinalizarin: A Novel Analogue of Anthracycline-Based Anticancer Agents Targets Human DNA Topoisomerase, Whereas Quinalizarin Itself Acts via Formation of Semiquinone on Acute Lymphoblastic Leukemia MOLT-4 and HCT 116 Cells

Sayantani Mukherjee Chatterjee,[†,⊥] Chetan Kumar Jain,[‡,§,#] Soumen Singha,[∥] Piyal Das,[†,¶] Susanta Roychoudhury,[‡,▽] Hemanta Kumar Majumder,[§] and Saurabh Das*[,†]

[†]Department of Chemistry (Inorganic Section) and [∥]Department of Physics, Jadavpur University, Kolkata 700032, India

[‡]Cancer Biology & Inflammatory Disorder Division and [§]Infectious Diseases and Immunology Division, Indian Institute of Chemical Biology, Kolkata 700032, India

Supporting Information

ABSTRACT: Quinalizarin (THAQ), a hydroxy-9,10-anthraquinone analogue of the family of anthracycline anticancer drugs and an inhibitor of protein kinase, was observed for its anticancer activity. Because apart from showing anticancer activity, anthracyclines and their analogues also show cardiotoxic side effects, believed to be addressed through metal complex formation; an effort was made to realize this by preparing a Co^{II} complex of THAQ. The aim of this study was to find out if complex formation leads to a decrease in the generation of intermediates that are responsible for toxic side effects. However, because this also meant that efficacy on cancer cells would be compromised, studies were undertaken on two cancer cell lines, namely, acute lymphoblastic leukemia (ALL) MOLT-4 and HCT116 cells. The complex decreases the flow of electrons from NADH to molecular oxygen (O_2) in the presence of NADH dehydrogenase forming less semiquinone than THAQ. It showed increased affinity toward DNA with binding constant values remaining constant over the physiological pH range unlike THAQ (for which decrease in binding constant values with increase in pH was observed). The complex is probably a human DNA topoisomerase I and human DNA topoisomerase II poison acting by stabilizing the covalent topoisomerase-cleaved DNA adduct, a phenomenon not observed for THAQ. Activity of the compounds on cancer cells suggests that THAQ was more effective on ALL MOLT-4 cells, whereas the complex performed better on HCT116 cells. Results suggest that the formation of semiquinone probably dominates the action because of THAQ, whereas the performance of the complex is attributed to increased DNA binding, inhibition of topoisomerase, and so forth. Inspite of a decrease in the generation of superoxide by the complex, it did not hamper efficacy on either cell line, probably compensated by improved DNA binding and inhibition of topoisomerase enzymes which are positive attributes of complex formation. A decrease in superoxide formation suggests that the complex could be less cardiotoxic, thus increasing its therapeutic index.

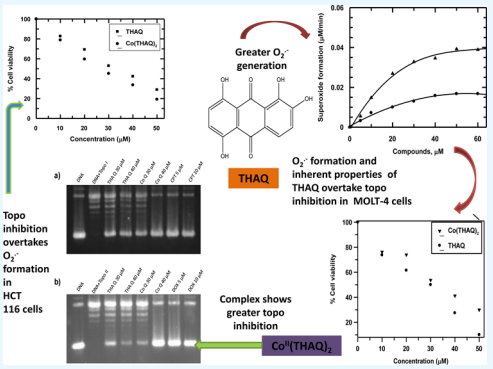

INTRODUCTION

Anthracyclines disrupt complex biological processes in their effort to be effective anticancer agents.[1−3] An important attribute of the molecules is their ability to interfere with human DNA topoisomerase I and human DNA topoisomerase II; enzymes that are intricately involved with DNA replication. Because anthracyclines are known to bind DNA through intercalation, it is important to understand the interactions that occur within cells.[4−11] The planar hydroxy-9,10-anthraquinone aglycon intercalates base pairs of DNA, whereas the amino sugar interacts with negatively charged phosphates in DNA major groove.[3,11] Intercalation brings about a change in the DNA double helix, affecting crucial cellular processes.[1−3,11] Efficacy of anthracyclines is also attributed to their ability to generate reactive free radicals. Growing evidence shows in vivo formation of semiquinone by one-electron reduction of the quinone that leads to a sequence of events important from a therapeutic point of view.[12−15] The formation of reactive intermediates is also responsible for dose-related cardiotoxicity.[3,11−15] Therefore, it is necessary to strike a balance between therapeutic efficacy and toxic side effects with regard to the generation of these reactive intermediates.[16,17] Research has revealed that metal complexes of anthracyclines modulate the formation of semiquinone that helps to control

Received: April 12, 2018
Accepted: July 23, 2018
Published: August 30, 2018

DOI: 10.1021/acsomega.8b00706
ACS Omega 2018, 3, 10255−10266

cardiotoxicity.[18−20] However, in controlling the formation of semiquinone through complex formation in an attempt to check cardiotoxicity, efficacy of the molecule is often compromised.

Two most popular drugs of the anthracycline family are daunomycin and adriamycin, natural products isolated from *Streptomyces peucetius* var. caesius that are in use for over five decades.[2,21] They are potent pharmaceutical ingredients requiring special care during production, isolation, and purification, making them very costly.[22,23] Hydroxy-9,10-anthraquinones present at the core of anthracyclines and essential for drug action would therefore be worth trying, to see if a hydroxy-9,10-anthraquinone on its own or as a metal complex shows efficacy comparable to anthracyclines.[1−3,12−15,22−27] Because slight variations in the location of hydroxy groups on an anthraquinone moiety of an anthracycline manifest in different ways in drug action, hence if different hydroxy-9,10-anthraquinones were investigated, they could help to identify and correlate a possible role for different hydroxy-9,10-anthraquinone units in these drug molecules.[28] This would enable us to achieve similar objectives using simpler molecules that are also less costly than anthracyclines.[22−30]

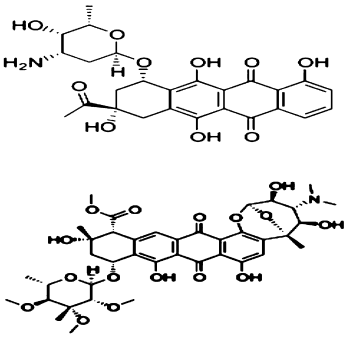

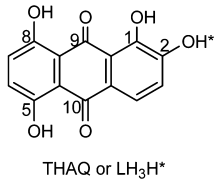

THAQ or LH_3H^*

CARMINOMYCIN (TOP) AND NOGALAMYCIN

We chose quinalizarin (THAQ) for its close similarity to anthracyclines such as carminomycin and nogalamycin. Besides, it has an ability to inhibit protein kinase CK2 (casein kinase 2);[31,32] CK2 exerts an antiapoptotic role by protecting regulatory proteins from caspase-mediated degradation, essential for cell viability.[33] Hence, we thought that THAQ could be an interesting starting point for investigating the role of hydroxy-9,10-anthraquinones because it already possesses certain attributes that are established with the help of biological investigations.[32−34] A Co^{II} complex was prepared to see the extent to which the activity of THAQ improved when bound to Co^{II} in the complex and the extent to which it resembles similar complexes of anthracyclines.[35]

RESULTS AND DISCUSSION

Physicochemical Studies on the Interaction of Co^{II} with THAQ. *Stoichiometry of Complex Formation by Mole Ratio and Job's Method.* The composition of the complex was determined by mixing different volumes of equimolar Co^{II} and THAQ. In the mole ratio method (Figure 1a), the concentration of Co^{II} was fixed, whereas that of THAQ was varied. Absorbance at 550 nm was plotted against $(T_L/T_M)_{T_M}$, and T_M and T_L are the concentrations of Co^{II} and THAQ, respectively. Intersection of two lines indicates the ratio at which THAQ binds Co^{II}. In Job's method of continuous variation (Figure 1b), complementary mixtures were prepared and the absorbance was recorded at 550 nm. This was plotted against volumes of THAQ or Co^{II}. Stoichiometry of Co^{II} to THAQ was found to be 1:2.

Proton Dissociation of THAQ In the Presence of Co^{II}. THAQ and Co^{II} were mixed in the ratio determined by mole ratio and Job's method. A spectrophotometric titration was performed in the pH range 3.0−11.0 (Figure S1, Supporting Information). Change in absorbance of THAQ at 560 nm in the presence of Co^{II} was fitted to eq 1 (Figure 2).

$$A_{obs} = A_1/(1 + 10^{pH-pK_1} + 10^{pH-pK_2}) + A_2/(1 + 10^{pK_1-pH} + 10^{pH-pK_2}) + A_3/(1 + 10^{pK_1-pH} + 10^{pK_2-pH}) \quad (1)$$

pK_1 and pK_2 were 4.77 ± 0.15 and 10.25 ± 0.05, respectively. Stability constant was determined using eqs S1−S5 (Supporting Information) and found to be 3.3×10^{19} ($\log \beta = 19.52$).

Characterization of $Co^{II}(THAQ)_2$. *UV−Vis Spectra of THAQ and $Co^{II}(THAQ)_2$.* The spectrum of the complex was recorded in dimethyl sulfoxide (DMSO), showing a peak at 554 nm. A slight red shift was observed in comparison to THAQ (taken in the aqueous medium, Figure S2, Supporting Information). λ_{max} for the complex appeared in the same range

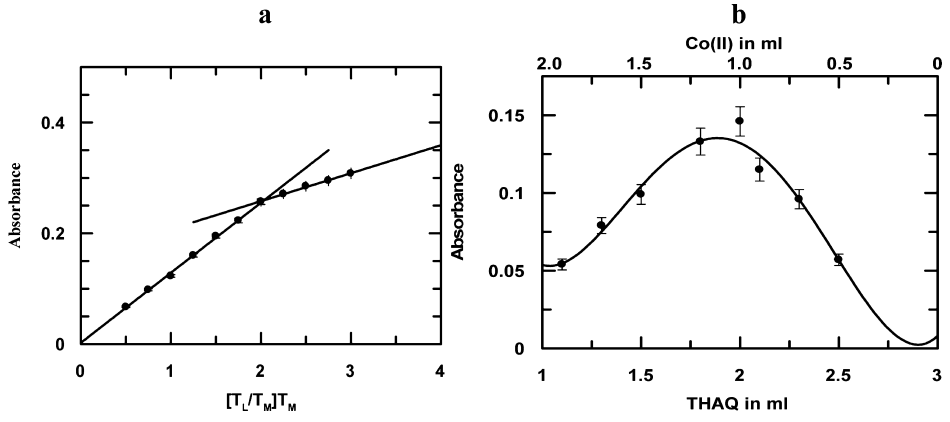

Figure 1. Plots showing gradual variation in absorbance at 550 nm for (a) change in [THAQ]/[Co^{II}] at a fixed concentration of Co^{II} = 10 μM and (b) continuous variation of THAQ and Co^{II} at physiological pH (~7.4). For (b), strength of stock solutions of Co^{II} and THAQ was 100 μM; each taken in a specific amount and diluted; [NaCl] = 10 mM, Temp. = 298 K.

DOI: 10.1021/acsomega.8b00706
ACS Omega 2018, 3, 10255−10266

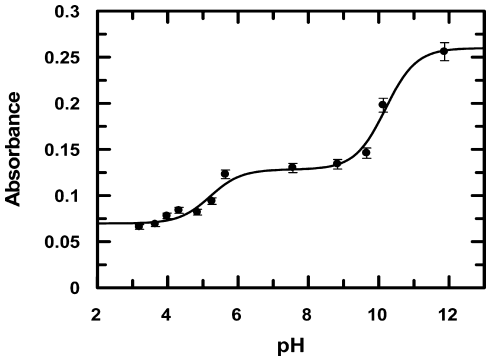

Figure 2. Spectrophotometric titration of THAQ in the presence of Co^{II} as shown by the variation in absorbance at 560 nm; [THAQ] = 20 μM, [Co^{II}] = 10 μM, [$NaNO_3$] = 10 mM, T = 301 K.

of wavelength as that used for physicochemical experiments involving Co^{II} and THAQ, suggesting that the prepared complex was similar to species that were formed during experiments performed in connection with the determination of stoichiometry.

IR of THAQ and $Co^{II}(THAQ)_2$. Infrared (IR) spectrum of THAQ revealed a sharp peak because of the stretching of phenolic-OH at 3379 cm^{-1} (Figure S3, Supporting Information) that changed to a broad band at 3434 cm^{-1} in the complex (Figure S4, Supporting Information).[36] Carbonyl stretching frequencies for THAQ at 1615 and 1581 cm^{-1} transformed to a broad peak at 1632 cm^{-1} in the complex. Peaks in the region from 1458 to 1093 cm^{-1} in the IR spectrum of THAQ (−OH and −CH bending) also underwent significant changes in the complex.

Mass Spectrum of the Complex. Mass spectra (MS) of the complex were recorded using two independent techniques (ESI^+ and EI^+). Combination of the two (Figure S5a,b, Supporting Information) helped to identify the molecular ion peak at m/z = 601.35. The peak at m/z = 553.36 was assigned to a fragment formed from the molecular ion, following loss of three −OH groups.

Magnetic Moment of $Co^{II}(THAQ)_2$. Magnetic susceptibility was measured by the Gouy method, and μ_{eff} was found to be 3.46 BM.

Electron Paramagnetic Resonance Spectroscopy. Electron paramagnetic resonance (EPR) spectroscopy measurement of the complex was done both in the solid state and in the DMF−ethanol mixture. The spectrum (Figure S6, Supporting Information) was assigned to high-spin (S = 3/2) Co^{II}. The line width broadening observed in the spectrum was the result of an interaction with neighboring Co^{II} ions as well as the outcome of recording the spectrum at room temperature.[37−39] An idea regarding a possible coordination around the metal center was obtained by comparing our spectrum with those reported earlier for similar Co^{II} complexes of adriamycin containing the hydroxy-9,10-anthraquinone unit or that of 1,4-dihydroxy-9,10-anthraquinone (quinizarin).[35−39] The EPR spectrum of the Co^{II} complex of quinizarin served as an important reference for our purpose.[37]

Thermogravimetric Analysis. Thermogravimetric analysis (TGA) suggests that the complex is stable up to 300 °C (Figure S7, Supporting Information).

On the Structure of the Complex. Single crystals of metal complexes of hydroxy-9,10-anthraquinones are rare with only one structure reported so far from single-crystal data.[40] Through previous work, we reported three structures of metal complexes of hydroxy-9,10-anthraquinones (purpurin and emodin) from powder diffraction data.[10,41,42] Attempts were made to obtain single crystals of the Co^{II} complex as well but we were not successful. We tried obtaining the structure from powder diffraction data but failed. Although the substance showed a reasonably clean powder diffraction data with distinctly different peaks for the complex, compared to that of the ligand, lack of peaks at low angles prevented us from arriving at a structure like we did earlier. Attempted calculations were not converging. Hence, we tried to arrive at the structure of the complex from the information obtained from other techniques, either in solid state or in solution. Emphasis was given to the analysis of mass spectrum data, information obtained from EPR and TGA. Using some of the instrument-based evidence, data obtained from physicochemical experiments such as pK_a and so forth and considering previous reports, a geometry optimization was attempted to arrive at a probable structure of the Co^{II}−THAQ complex.[35−39] Similar to that reported earlier for Co^{II} complexes of the drug adriamycin and Co^{II} complexes of quinizarin (another hydroxy-9,10-anthraquinone), our complex was believed to have tetragonal coordination because EPR characteristics obtained were similar to those reported earlier.[37−39] Spectral features with broad signals resemble those for complexes with tetragonal coordination for Co^{II} complexes of 3-formylsalicylic acid-$R(NH_2)_2$ Schiff bases.[43] The broad signals could be due to the complex having a tetragonal coordination structure as observed in DMF−ethanol.

THAQ has a planar geometry. The thermal analysis plot (TGA pattern) does not indicate the presence of any coordinated or even guest water molecules. Therefore, the possibility of the Co^{II} complex having an octahedral geometry is ruled out. Hence, two possibilities that remain based on the experimental evidence are either tetrahedral or square planar coordination. Literature survey suggests when a metal ion has d^7 configuration and binds to strong field ligands, it forms a square planar architecture but when coordinated to weak field ligands shows tetrahedral coordination. $Cobalt^{II}$ in a THAQ complex has a d^7 configuration. When THAQ binds Co^{II}, one attachment is through the C═O group having vacant π^* orbitals capable of participating in back donation at the site of coordination. Hence, it might act as a mildly strong field ligand and probably not too strong either. We considered two model structures for $Co^{II}(THAQ)_2$. In the first, Co^{II} was considered to be coordinated by two THAQs in a tetrahedral arrangement and in another (the second model), coordination environment was considered square planar. We then performed geometry optimization in the gaseous state using Gaussian 09 package and the very basic semiempirical method with unrestricted PM6 basis set to investigate which one of the two structures was lower in energy in their respective ground states, assuming that the lower energy configuration tends to give the more favored structure.[44] The first model failed to converge even after running a sufficiently large number of cycles. It could not generate any output. However, the second model provided an optimized geometry with energy −15.2075 eV for the ground state with no imaginary frequencies. The optimized geometry is presented in Figure 3 with a few selected bond lengths and bond angles listed in Table 1. The optimized geometry shows the metal center coordinated in a square planar fashion.

Although two THAQ ligands are parallel to each other, they are however not in the same plane (geometry optimized

DOI: 10.1021/acsomega.8b00706
ACS Omega 2018, 3, 10255−10266

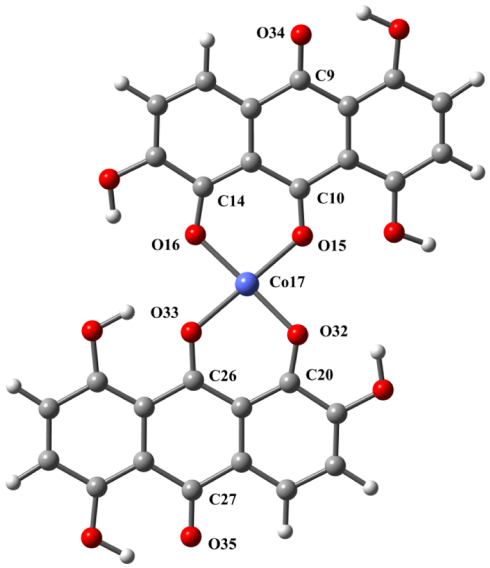

Figure 3. Optimized structure of $Co^{II}(THAQ)_2$ having square planar coordination geometry.

Table 1. Some Selected Bond Lengths and Bond Angles for $Co^{II}(THAQ)_2$

Co17−O15	1.927	C27−O35	1.232
Co17−O16	1.884	C9−O34	1.231
Co17−O33	1.936	O32−Co17−O33	92.95
Co17−O32	1.887	O15−Co17−O16	93.98
C26−O33	1.272	C14−O16−Co17	120.58
C20−O32	1.293	C10−O15−Co17	124.80
C10−O15	1.255	C20−O32−Co17	121.92
C14−O16	1.299	C26−O32−Co17	125.33

structure in the Supporting Information). It may be seen in the geometry optimized structure (Supporting Information) that the angles made by the ligating O atoms of THAQ with Co^{II} are not perfectly 90°. While two of them are ∼93° and 94°, the other two are ∼88°. Therefore, a slight distortion is present even in square planar geometry. Keeping in mind the aspect of vacant π^* orbitals of the coordinating C═O group and a possibility for back donation at the site of coordination, there is developed a tendency to form a square planar configuration rather than tetrahedral or a structure in between the two; hence, a distortion was obtained in square planar geometry as well.

Similar calculations were performed for geometry computed in DMSO solvent simulated by a conductor-like polarizable continuum model (CPCM). The UV−vis transition of the complex was computed by a single-point calculation carried out using a time-dependent density functional theory method starting with the ground state geometry optimized in DMSO media. Unrestricted Becke's three-parameter hybrid functional and Lee−Yang−Parr's gradient-corrected correlation functional (UB3LYP) along with 6-311+G(d,p) basis set were adopted for C, H, and O. For Co, we chose the LanL2DZ basis set. Excitation energies computed in the DMSO solvent simulated by the CPCM were determined by using the nonequilibrium approach that was designed for the study of the absorption processes. Only singlet−singlet transitions, that are spin-allowed transitions, were taken into account. The theoretical UV−vis spectrum of the complex obtained in DMSO is shown in Figure S8. It has very close similarity to the experimentally obtained UV−vis spectrum of the complex in DMSO (Figure S2) and with the spectra obtained in aqueous solution when pH metric titration of THAQ was attempted in the presence of Co(II) (Figure S1). This information further supports that the geometry of the complex is square planar with minor distortions.

Interaction of $Co^{II}(THAQ)_2$ with Calf Thymus DNA. Using UV−Vis Spectroscopy. The complex (50 μM) was titrated with calf thymus DNA to saturation. A decrease in absorbance at 550 nm at pH 7.4 was attributed to intercalation between base pairs of DNA (Figure 4).[25−29] Similar titrations were performed at pH 6.8 and 8.2. Figure S9 is a typical double reciprocal plot obeying eq 3. Figure 5 is a plot of $\Delta A/\Delta A_{max}$ against concentration of DNA fitted by nonlinear square fit analysis (eqs 4 and 5) for a titration performed at pH 6.8. Similar nonlinear fitting was done for titrations performed at other pH values. Values for K_{app} are summarized in Table 2. The inset of Figure 5 shows determination of n_b (Table 2). Overall binding constant values (K') were obtained by multiplying K_{app} with n_b for all titrations performed at different pHs (Table 2).

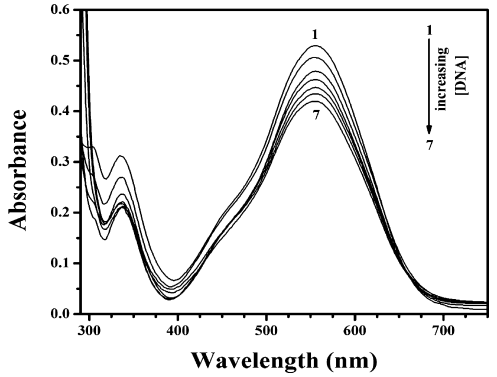

Figure 4. Absorption spectra of 50 μM $Co^{II}(THAQ)_2$ in the absence (1) and presence of different concentrations of calf thymus DNA (2) 42.83, (3) 85.45, (4) 127.86, (5) 212.05, (6) 336.79, and (7) 454.71 μM; [NaCl] = 120 mM, pH = 7.4, Temp. = 298 K.

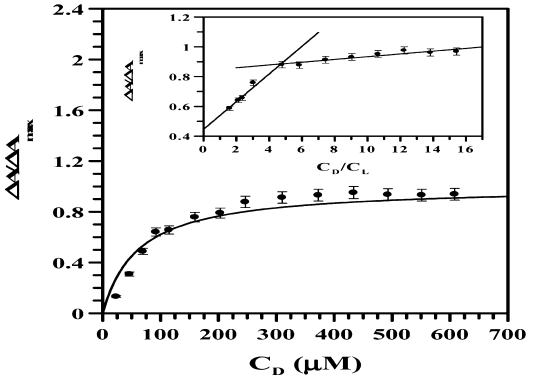

Figure 5. Binding isotherm for interaction of $Co^{II}(THAQ)_2$ with calf thymus DNA where $\Delta A/\Delta A_{max}$was plotted against the concentration of DNA. The dark line represents the fitted data obeying eq 5. [$Co^{II}(THAQ)_2$] = 50 μM, [NaCl] = 120 mM; pH = 6.8; Temp. = 301 K. Inset: Plot of normalized increase in absorbance as a function of the mole ratio of calf thymus DNA to $Co^{II}(THAQ)_2$.

Data from the titrations at three different pHs were also analyzed according to the modified form of the Scatchard

DOI: 10.1021/acsomega.8b00706
ACS Omega 2018, 3, 10255−10266

Table 2. Binding Parameters for the Interaction of $Co(THAQ)_2$ with Calf Thymus DNA at Different pHs

monitoring technique	pH	apparent binding constants $K_{app} \times 10^{-4}$ (M^{-1}): from double reciprocal plot	apparent binding constants $K_{app} \times 10^{-4}$ (M^{-1}): from nonlinear fit	site size (n_b) from mole ratio plot	overall binding constant $K^* \times 10^{-5}$ (M^{-1}) [$K^* = K_{app} \times n_b$]	overall binding constant $K' \times 10^{-5}$ (M^{-1}) (from Scatchard plot)	site size ($n_b = n^{-1}$) from Scatchard plot	overall binding constant from double reciprocal plot with intercept = 1 (eq 6) $K^* \times 10^{-5}$ (M^{-1})
UV−vis	6.8	3.85	3.75	4.0	1.52	1.51	3.70	1.03
	7.4	4.07	3.88	4.2	1.67	2.03	3.53	1.41
	8.2	4.01	4.32	4.2	1.75	2.14	3.67	1.54
fluorescence	7.4	3.70	3.90	4.0	1.52	1.74	3.80	2.30

equation (eq 6), providing values for overall binding constant (K') and n ($=n_b^{-1}$).[45] A typical Scatchard plot for the complex at pH 8.2 is shown in Figure 6. Results of similar plots at other

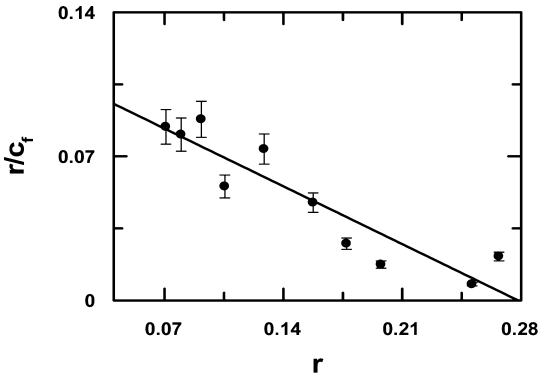

Figure 6. Scatchard plot for the interaction of $Co^{II}(THAQ)_2$ with calf thymus DNA. [$Co^{II}(THAQ)_2$] = 50 μM, [NaCl] = 120 mM, pH = 8.2, temperature = 301 K.

pH are summarized in Table 2. An interesting observation made from the study on DNA binding with regard to evaluation of site size (n_b) for $Co^{II}(THAQ)_2$ binding to calf thymus DNA was that the value was almost double that obtained for THAQ itself binding to DNA. This serves as yet another evidence that two molecules of THAQ are bound to Co^{II} in the complex.[26−28]

Data obtained at all three pHs were analyzed using eq 7. Apparent and overall binding constants were evaluated (Table 2). Figure S10 is a typical plot obtained by fitting the titration data to eq 7 at pH 8.2. Binding constant and site size of interaction (n_b) for the complex interacting with DNA evaluated from different approaches not only corroborate each other but also indicate that they are higher than THAQ.[25] Unlike THAQ, binding constant values for the complex did not decrease with the increase in the pH of the medium.[29] This is significant for it indicates that complex formation is able to prevent the generation of anionic species on THAQ at physiological pH which was responsible for the decrease in binding constant values for THAQ interacting with DNA at high pH.[29] The result is significant from a biological point of view as well because cancer patients show fluctuation of pH in body fluids, a matter of concern regarding the application of several drugs.[46] Therefore, if this complex is ever developed into a drug, it may be expected that its activity based on DNA interaction would remain more or less same over a considerable range of pH, an improvement over THAQ.

Figure 7 relates the ratio of input drug/DNA (r_i) to the ratio of bound drug/DNA (r_b) as derived from Scatchard

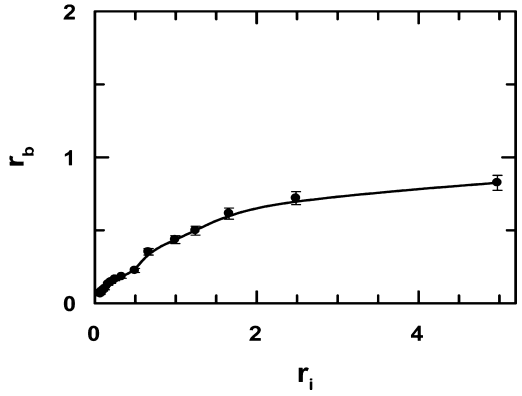

Figure 7. Relationship of input $Co^{II}(THAQ)_2$/DNA (r_i) to bound $Co^{II}(THAQ)_2$/DNA (r_b) as calculated from the decrease in absorbance, following interaction of $Co^{II}(THAQ)_2$ with calf thymus DNA at pH 7.4 in a medium having 120 mM NaCl.

calculations.[45,47] For such a plot, a 45° line suggests that the entire compound present was bound to DNA.[47] Plots obtained at all three pHs were close to each other, suggesting once again that binding of $Co^{II}(THAQ)_2$ to calf thymus DNA is not much influenced by pH.

Using Fluorescence Spectroscopy. Binding constant and site size of interaction of the complex were also determined using fluorescence spectroscopy (Figure 8) at pH 7.4. The data

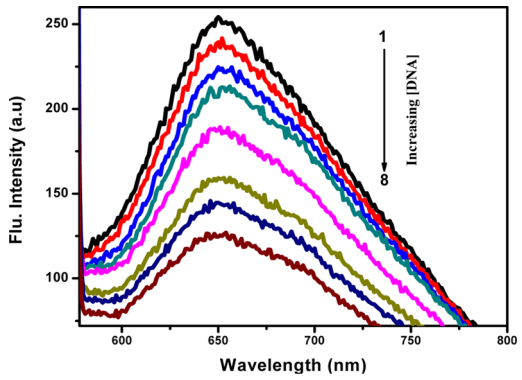

Figure 8. Fluorescence spectra of 100 μM $Co^{II}(THAQ)_2$ in the absence (1) and presence of different concentrations of calf thymus DNA (2) 97.01, (3) 193.07, (4) 382.35, (5) 567.96, (6) 750, (7) 928.57, and (8) 1103.77 μM. [NaCl] = 120 mM, pH = 7.4, T = 298 K.

DOI: 10.1021/acsomega.8b00706
ACS Omega 2018, 3, 10255−10266

was analyzed using eqs 2−6. A double reciprocal plot (Figure S11) yields values for K_{app} and ΔF_{max}. Nonlinear square fit analysis (Figure S12) provides another value for K_{app} (Table 2). The data were analyzed according to the modified Scatchard equation [eq 6] and Figure S13 (Supporting Information) and fitted to eq 7 (Figure S14). Overall binding constant (K') and site size (n) were determined (Table 2).

NADH Dehydrogenase Assay. Formation of superoxide radical anion catalyzed by THAQ and $Co^{II}(THAQ)_2$ was measured from reduction of cytochrome *c* inhibited by superoxide dismutase (SOD) in the presence of NADH and NADH dehydrogenase (Figure 9).[19,24,48−50] In such enzyme-

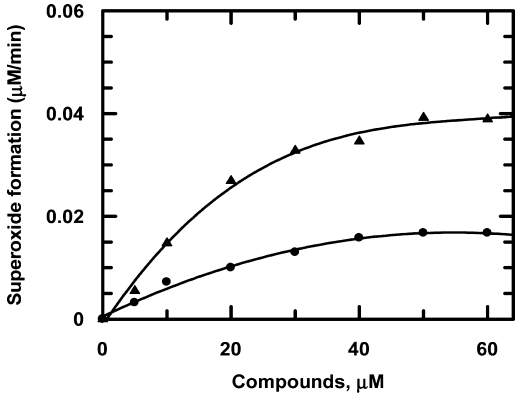

Figure 9. Effect of THAQ and $Co^{II}(THAQ)_2$ on superoxide formation by NADH dehydrogenase. Superoxide formation was determined with the help of a spectrophotometer as rate of SOD-inhibitable cytochrome *c* reduction. The reaction mixture contained 100 mM (4-(2-hydroxyethyl)-1-piperazineethanesulfonic acid) (HEPES) buffer (pH 7.2), 80.0 μM cytochrome *c*, 157.5 μM NADH, 3 U L^{-1} NADH dehydrogenase, 0 or 40.0 μg mL^{-1} SOD, and the indicated amount of compound [▲, THAQ; ●, $Co^{II}(THAQ)_2$].

assisted reactions, superoxide radical anions are produced when semiquinone radical anions are oxidized by molecular oxygen. Owing to complex formation, because one of the carbonyls of THAQ is engaged in coordinating Co^{II}, it is only at the other carbonyl that a semiquinone can form explaining why a decrease is observed following complex formation. This gets manifested as decreased superoxide formation (Figure 9). Even when the semiquinone radical anion forms at the free carbonyl of one of the two bound THAQ molecules, the metal ion present in the complex is quick to withdraw the electron toward itself by more than one mechanism further decreasing the possibility of $Co^{II}(THAQ)_2$ existing as $Co^{II}(THAQ)(THAQ^{\bullet-})$.[51]

Hence, there is substantial decrease in the possibility of interaction of a semiquinone formed on the complex with molecular oxygen justifying low yields of superoxide (Figure 9). Information available in the literature suggests when anthracyclines are complexed with metal ions, they decrease semiquinone formation and that most complexes have reduced cardiotoxic side effects.[4,19,20,52,53] Working with hydroxy-9,10-anthraquinones and their complexes with 3d transition-metal ions, we too observed a substantial decrease in semiquinone formation.[42,54] In the case of some iron complexes, however, or for situations of iron overload, there is an increase in semiquinone formation for which the reason is completely different.[53−55] Because THAQ closely resembles the core of anthracyclines that are responsible for the generation of semiquinone or superoxide, hence like that reported for complexes of anthracyclines, complexes of hydroxy-9,10-anthraquinones, say THAQ, should also show decreased cardiotoxic side effects if tried in cancer chemotherapy.[3,12−15,18−20] Metal ions such as Fe(III) and Cu(II) having a stable lower oxidation state, complexes are both an efficient $O_2^{\bullet-}$ quencher and effective cytotoxic agents owing to their ability to form $^{\bullet}OH$ [details in the Supporting Information].[53−57] However, for the Co^{II} complex of THAQ, Co^{I} not being that much stable, mechanism leading to the generation of $^{\bullet}OH$ is unlikely. Therefore, the probability of the Co^{II} complex acting as a cytotoxic agent making use of the redox mechanism is not very high.

In Vitro Activity of THAQ and $Co^{II}(THAQ)_2$ on Human DNA Topoisomerase Enzymes. The inhibitory effect of THAQ and $Co^{II}(THAQ)_2$ was studied with the help of a DNA relaxation assay on recombinant human DNA topoisomerase enzymes in the absence and presence of the compounds. A relaxation assay such as this is based on the fact that supercoiled DNA molecules are relaxed by active topoisomerases, leading to the formation of topoisomers of relaxed DNA. These topoisomers migrate slowly compared to supercoiled plasmid DNA in agarose gel. Hence, the activity of topoisomerase may be checked by observing gel bands for relaxed topoisomers. When the topoisomerase is somehow inhibited, bands for relaxed topoisomers do not appear on the gel. In our case, we found that at concentrations of 10 or 20 μM, both THAQ and $Co^{II}(THAQ)_2$ were unable to influence or inhibit the action of either human DNA topoisomerase I or human DNA topoisomerase II as realized from their relaxation activities. However, at a concentration of 30 μM, inhibition due to $Co^{II}(THAQ)_2$ sets in, whereas no inhibition was observed for THAQ. At 40 μM, $Co^{II}(THAQ)_2$ completely inhibits human DNA topoisomerase I and human DNA topoisomerase II relaxation activities with THAQ still not showing any effect (Figure 10a,b). Role of aqueous Co^{II} taken in the form of $CoCl_2$ was also checked to find out if it might be responsible for inhibiting either human DNA topoisomerase I or human DNA topoisomerase II. Experiments reveal neither aqueous Co^{II} nor THAQ had any inhibitory effect on the topoisomerase enzymes up to 40 μM (Figure 10a,b). It may therefore be said with a lot of certainty that the complex poisons the enzymes by stabilizing a covalent enzyme-DNA adduct, trapping the enzyme in a DNA-linked condition, being an attribute of complex formation.

Inhibitory effects were also checked for migration of substrate DNA using standard compounds such as CPT (a control for topoisomerase I inhibition) and DOX (a control for topoisomerase II inhibition) at two different concentrations (Figure 10a,b). These showed no DNA migration, indicating complete inhibition of the respective topoisomerase enzymes. kDNA decatenation assay for DNA topoisomerase II in the presence and absence of THAQ and $Co^{II}(THAQ)_2$ showed that the complex inhibits decatenation activity of human DNA topoisomerase II at 40 μM, whereas THAQ had no effect. Although the active concentration for $Co^{II}(THAQ)_2$ was much higher than CPT and DOX, experimental evidence suggest that $Co^{II}(THAQ)_2$ is a potent dual inhibitor of human DNA topoisomerase I and human DNA topoisomerase II enzymes in vitro.

Effect of THAQ and $Co^{II}(THAQ)_2$ on Two Different Cancer Cells. An 3-(4,5-dimethylthiazol-2-yl)-2,5-diphenyltetrazolium bromide (MTT) assay was performed using THAQ and

DOI: 10.1021/acsomega.8b00706
ACS Omega 2018, 3, 10255−10266

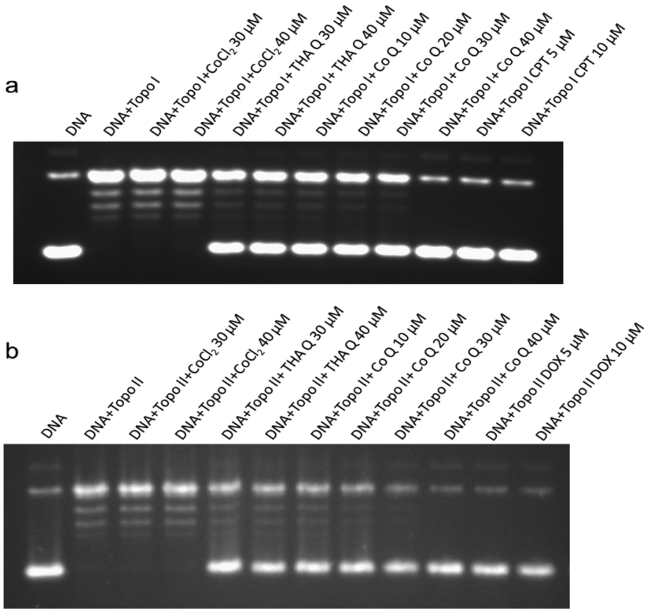

Figure 10. DNA topoisomerase relaxation assays. (a) DNA topo I relaxation assay. Lane 1 is 100 fmol supercoiled pBS (SK^+) DNA; lane 2 is 100 fmol supercoiled pBS (SK^+) DNA with 50 fmol topoisomerase I enzyme; lane 3 is same as lane 2 but with 30 μM $CoCl_2$; lane 4 is same as lane 2 but with 40 μM $CoCl_2$; lane 5 is same as lane 2 but with 30 μM THAQ; lane 6 is same as lane 2 but with 40 μM THAQ; lane 7 is same as lane 2 but with 10 μM$Co^{II}(THAQ)_2$; lane 8 is same as lane 2 but with 20 μM$Co^{II}(THAQ)_2$; lane 9 is same as lane 2 but with 30 μM$Co^{II}(THAQ)_2$; lane 10 is same as lane 2 but with 40 μM $Co^{II}(THAQ)_2$; lane 11 is same as lane 2 but with 5 μM camptothecin (CPT); and lane 12 is same as lane 2 but with 10 μM CPT. All reactions were incubated at 37 °C for 30 min and analyzed by agarose gel electrophoresis. (b) DNA topo II relaxation assay. Lane 1 is 100 fmol supercoiled pBS (SK^+) DNA; lane 2 is 100 fmol supercoiled pBS (SK^+) DNA with 50 fmol topoisomerase II enzyme; lane 3 is same as lane 2 but with 30 μM $CoCl_2$; lane 4 is same as lane 2 but with 40 μM $CoCl_2$; lane 5 is same as lane 2 but with 30 μM THAQ; lane 6 is same as lane 2 but with 40 μM THAQ; lane 7 is same as lane 2 but with 10 μM$Co^{II}(THAQ)_2$; lane 8 is same as lane 2 but with 20 μM$Co^{II}(THAQ)_2$; lane 9 is same as lane 2 but with 30 μM$Co^{II}(THAQ)_2$; lane 10 is same as lane 2 but with 40 μM$Co^{II}(THAQ)_2$; lane 11 is same as lane 2 but with 5 μM doxorubicin (DOX); and lane 12 is same as lane 2 but with 10 μM DOX. All reactions were incubated at 37 °C for 30 min and analyzed by agarose gel electrophoresis.

$Co^{II}(THAQ)_2$ on acute lymphoblastic leukemia (ALL) MOLT-4 cells and HCT116 cells. Results suggest that THAQ (IC_{50} = 28.0 μM) was slightly better in performance than $Co^{II}(THAQ)_2$ (IC_{50} = 33.0 μM) on ALL MOLT-4 cells (Figure 11a), whereas $Co^{II}(THAQ)_2$ (IC_{50} = 27.0 μM) was better than THAQ (IC_{50} = 31.5 μM) on HCT116 cells (Figure 11b). In a previous study, we showed cell killing by the Cu^{II} complex of purpurin where it was thought to be a consequence of inhibition of human DNA topoisomerase I and human DNA topoisomerase II present in the nucleus of MOLT-4 cells.[10] In that report, efficacy shown by the Cu^{II} complex on inhibition of topoisomerase over that of purpurin had the same trend as the performance of the compounds on ALL MOLT-4 cells.[10] However, in the present study, although $Co^{II}(THAQ)_2$ was more effective than THAQ in inhibiting human DNA topoisomerase I and human DNA topoisomerase II and also better with respect to binding DNA, results on MOLT-4 cells suggest that the performance of the complex was somewhat weaker than THAQ [according to obtained IC_{50} values (Figure 11a)] which is not unusual as reports exist in the literature showing metal anthracyclines as less efficient than the parent compound.[20,58]

This is possible if cell killing by THAQ due to reactive oxygen species (ROS) generation more than outweighs the ability of the complex to affect cells due to topoisomerase inhibition, keeping in mind the fact that the complex is unlikely to succeed by the radical formation mechanism because ROS generation by it is much less (Figure 9, Table 3). Although the difference in IC_{50} values is small, the result may be believed as it is the outcome of four independent experiments. At this stage, it would be important to remember THAQ has another attribute apart from ROS generation; it possesses an inhibitory action on protein kinase CK2 which could well affect cell viability in ALL MOLT-4 cells. Hence, THAQ with two attributes (protein kinase CK2 inhibition and ROS generation) could just be better than the complex on ALL MOLT-4 cells.[29,30,58] Performance of the compounds on HCT116 cells was however in line with our previous results obtained for purpurin and its Cu^{II}complex, that is, $Co^{II}(THAQ)_2$ more effective than THAQ (Figure 11b).[10] This indicates that for HCT116 cells, inhibition due to human DNA topoisomerase I and human DNA topoisomerase II probably dominates over the ROS generation mechanism that keeps the complex ahead. Compounds CPT, etoposide (ETO), and DOX were used as controls for the experiment. IC_{50} values for CPT was 1.5 μM, and for ETO, it was 1.0 μM and for DOX, 1.0 μM. Results were also compared with the performance of cisplatin on the same cell lines.[59−62]

CONCLUSIONS

$Co^{II}(THAQ)_2$ shows enhanced binding with calf thymus DNA compared to THAQ. An important outcome of the study on the binding of the complex with DNA was that unlike THAQ, binding constant values for the complex did not decrease with an increase in the pH of the medium. This can be considered a marked improvement over THAQ and was possible because $Co^{II}(THAQ)_2$, unlike THAQ, does not form anionic species in solution at physiological pH that affects binding with DNA. Hence, the complex could be effective on cancer patients whose body fluids show fluctuation in pH. Because cancer cells are reported to thrive at low pH and are uncomfortable under alkaline conditions, increasing the pH of body fluids of cancer patients is a form of treatment. $Co^{II}(THAQ)_2$ could be important as a drug for treatment at high pH where many have problems. Therefore, with decreased superoxide formation, increased affinity toward DNA, and the capability to inhibit the action of topoisomerase enzymes, $Co^{II}(THAQ)_2$ could just be an important candidate for anticancer activity having lesser possibility for toxic side effects. Results on topoisomerase inhibition enable the complex to be an effective anticancer agent, supported by its performance on ALL MOLT-4 and HCT 116 cells adding to an emerging field of trying inorganic complexes as anticancer drugs.[35,62] Our results are also in agreement with a recent report on the participation of different metal ions in doxorubicin complexes found to be active on MCF-7 breast cancer cells.[35]

EXPERIMENTAL PROCEDURES

Materials and Preparation of Solutions. THAQ was purchased from BDH, England, and purified by re-crystal-

DOI: 10.1021/acsomega.8b00706
ACS Omega 2018, 3, 10255−10266

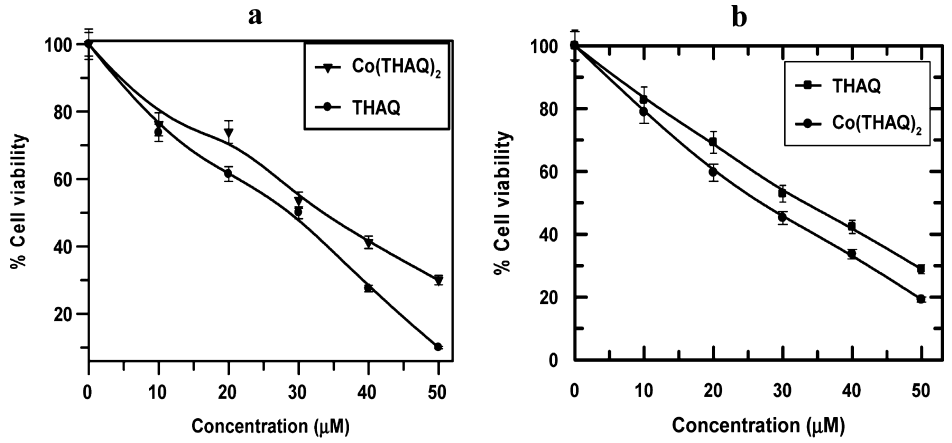

Figure 11. Plots showing dose response curves for the effect of THAQ and $Co^{II}(THAQ)_2$ on (a) ALL MOLT-4 cells and (b) HCT 116 cells treated with each compound for 72 h and thereafter MTT assay performed.

Table 3. Comparison of the Findings of $O_2^{\bullet-}$ Generation/Topoisomerase Inhibition with the IC_{50} Values of THAQ and $Co^{II}(THAQ)_2$ on ALL MOLT-4 and HCT 116 Cells

compounds	generation of $O_2^{\bullet-}$ in NADH dehydrogenase assay (Figure 9) (μM/min)	MIC for topoisomerase I inhibition	MIC for topoisomerase II inhibition	IC_{50} for ALL MOLT-4 cells	IC_{50} for HCT 116 cells
THAQ	0.039 at 60.0 μM	>40.0 μM	>40.0 μM	28.0 μM	31.5 μM
$Co^{II}(THAQ)_2$	0.017 at 60.0 μM	40.0 μM	40.0 μM	33.0 μM	27.0 μM
cisplatin[a]				(0.3−1.3) μM	(5.4−7.4) μM
doxorubicin				1.0 μM	

[a]The data for cisplatin provided in the table were taken from the literature to be able to compare the performance of $Co^{II}(THAQ)_2$ with a standard anticancer agent.[59−62]

lization from the alcohol−water mixture. Hydroxy-9,10-anthraquinone, which is sensitive to light and oxygen, solutions were prepared just before use or stored in dark bottles under deaerated condition. $CoCl_2 \cdot 6H_2O$ [Merck, India] was dissolved in deionized triple-distilled water. Calf thymus DNA, purchased from Sisco Research Laboratories, India, was dissolved in phosphate buffer and kept for a minimum of 24 h. Its concentration was determined in terms of nucleotide at 260 nm considering ε_{260} to be 6600 M^{-1} cm^{-1}. Absorbance at 260 and 280 nm was used to calculate the ratio $[1.8 < A_{260}/A_{280} > 1.9]$ that indicates DNA to be sufficiently free of protein. Quality of the calf thymus DNA used was also checked from the characteristic circular dichroism band at 260 nm. Phosphate buffer containing 120 mM NaCl, 3.5 mM KCl, 1 mM $CaCl_2$, and 0.5 mM $MgCl_2$ was prepared to maintain pH in the physiological pH range (6.8−8.2) during titration of the complex with DNA. Recombinant human DNA topoisomerase I and human DNA topoisomerase II alpha were purchased from TopoGENInc (Port Orange, Florida, USA).

Methods. *Instrumental Techniques.* Absorption spectra related to complex formation and DNA titration were recorded on a JASCO V-630 spectrophotometer. Fourier transform infrared spectroscopy of the solid complex was recorded on a PerkinElmer RX-I spectrophotometer using KBr pellets. Mass spectrum was recorded on Micromass Q-Tof micro, Waters Corporation. Elemental analysis was done on a PerkinElmer 2400 Series-II CHN analyzer. EPR spectrum was recorded on a JEOL JES-FA 200 ESR spectrophotometer. DNA binding studies using fluorescence were done on a RF-530 IPC spectrofluorophotometer, Shimadzu. Enzyme assay was performed on a JASCO V-630 spectrophotometer using the kinetics software of the instrument.

Preparation of $Co^{II}(THAQ)_2$. A solution of THAQ (0.0054 g) in methanol (100 mL) was added to a solution of $CoCl_2$ (0.0024 g) in 0.2 M aqueous $NaNO_3$ (100 mL). pH was adjusted to 5.5, and the mixture was warmed under reflux for 4 h. After two weeks, a compound having a reddish violet color appeared following slow evaporation of the solvent. It was filtered and recrystallized.

Anal. Calcd (%) for $C_{28}H_{14}O_{12}Co$: C, 55.87; H, 2.33. Found: C, 55.12; H, 2.35. Molecular ion peak (M) at 601.35; $[M - 3(OH)]^+$ = 553.36; λ_{max} = 554 nm in DMSO.

DNA Binding. Interaction of the complex with calf thymus DNA was followed considering the following equilibrium (eq 2).

$$L + DNA \rightleftharpoons L{-}DNA \qquad K_d = \frac{[L][DNA]}{[L{-}DNA]} \tag{2}$$

L represents the complex, and K_d is the dissociation constant[25−27,29] whose reciprocal is the apparent binding constant (K_{app}). Equation 3 was obtained from eq 2 where reciprocal of the change in absorbance or fluorescence was plotted against reciprocal of $(C_D - C_0)$. C_D refers to the concentration of calf thymus DNA, and C_0 is the concentration of the complex. For fluorescence experiments, the complex was excited at 560 nm and emission recorded at 650 nm. Using eq 3, ΔA_{max} and K_{app} (K_d^{-1}) were determined from the intercept and slope, respectively.

$$\frac{1}{\Delta A} = \frac{1}{\Delta A_{max}} + \frac{K_d}{\Delta A_{max}(C_D - C_0)} \tag{3}$$

ΔA represents the change in absorbance of the complex following interaction with DNA. ΔA_{max} is the maximum change in absorbance for each titration. For fluorescence

DOI: 10.1021/acsomega.8b00706
ACS Omega 2018, 3, 10255−10266

experiments, ΔA and ΔA_{max} of eq 3 were ΔF and ΔF_{max}, respectively.

$$K_d = \frac{\left[C_0 - \left(\frac{\Delta A}{\Delta A_{max}}\right)C_0\right]\left[C_D - \left(\frac{\Delta A}{\Delta A_{max}}\right)C_0\right]}{\left(\frac{\Delta A}{\Delta A_{max}}\right)C_0} \quad (4)$$

$$C_0\left(\frac{\Delta A}{\Delta A_{max}}\right)^2 - (C_0 + C_D + K_d)\left(\frac{\Delta A}{\Delta A_{max}}\right) + C_D = 0 \quad (5)$$

$\Delta A/\Delta A_{max}$ or $\Delta F/\Delta F_{max}$ was plotted against C_D. Equations 4 and 5 were used to fit the data according to nonlinear square fit analysis providing another value for apparent binding constant.[25−27,29] Titration of the complex with DNA was analyzed according to a modified form of the Scatchard equation [eq 6]. Overall binding constant (K') and site size (n) were determined.[45]

$$r/C_f = K'(n - r) \quad (6)$$

$r = C_b/C_D$; C_b is the concentration of the bound form of the complex, and C_f is the free form. "n" provides binding stoichiometry in terms of bound complex per nucleotide, whereas "n_b" reciprocal of "n" provides binding site size in terms of the number of nucleotides bound to the complex. "n_b" was obtained by plotting $\Delta A/\Delta A_{max}$ or $\Delta F/\Delta F_{max}$ against C_D/[complex]. K' was obtained by multiplying K_{app} with "n_b". Values of K' obtained in this manner from UV−vis and fluorescence spectroscopy were compared with that obtained directly from Scatchard plots. The titrimetric data were fitted to another form of a double reciprocal plot having intercept on y axis = 1 (eq 7)

$$\frac{1}{(C_b/C_0)} = 1 + \frac{1}{[K][C_D]} \quad (7)$$

This equation provides another value for the apparent binding constant (K_{app}) for interaction of the complex with DNA which when multiplied by n_b provides overall binding constant (K').

NADH Dehydrogenase Assay. An enzyme assay was performed at 298 K with cytochrome c as an electron acceptor.[48] Both THAQ and $Co^{II}(THAQ)_2$ were tried in NADH-cytochrome c reductase activity where reduction of cytochrome c was followed at 550 nm. In the assay, performed at pH 7.4 (0.05 M HEPES buffer), the concentration of THAQ and $Co^{II}(THAQ)_2$ was varied from 0 to 50.0 μM. Activity of NADH dehydrogenase was expressed in units where one unit of activity reduces 1.0 μmol oxidized cytochrome c per minute at pH 7.4 at 298 K.

DNA Relaxation Assays for Topoisomerase I and Topoisomerase II. DNA relaxation assays for recombinant human DNA topoisomerase I and human DNA topoisomerase II were performed in the absence and presence of THAQ and the complex by briefly incubating 100 fmol supercoiled pBS SK (+) DNA with 50 fmol enzyme in buffer, provided with the enzymes. The reaction buffer contained 5 mM dithiothreitol as the reducing agent. DMSO concentration was maintained at 0.5% (vehicle control). Reactions were incubated at 37 °C for 30 min and loaded on 1% agarose gel. It was thereafter electrophoresed overnight at 20 V. On completion of electrophoresis, gels were stained with 0.5 μg mL^{-1} ethidium bromide and viewed by Gel Doc 2000 (BioRad) under UV illumination. Relaxation was realized by monitoring the decreased electrophoretic mobility of relaxed topoisomers of pBS SK (+) DNA.

Cell Culture. HCT 116 and MOLT-4 cells were cultured in McCoy's 5A media (GIBCO, Invitrogen, Carlsbad, CA, US) and RPMI-1640 media (GIBCO, Invitrogen, Carlsbad, CA, US), respectively. Media were supplemented with 10% fetal bovine serum (GIBCO), antibiotic mixture 1× penicillin−streptomycin−neomycin (GIBCO), and gentamicin reagent solution (GIBCO). Cells were incubated in a humidified CO_2 incubator at 37 °C.

Cell Viability Assay. Cells were seeded on a 96-well plate one day prior to compound addition. They were treated with compounds dissolved in DMSO. DMSO concentration was less than 0.5%. After 48 h of incubation, cells were washed with 1× phosphate-buffered saline and treated with MTT for 4 h at 37 °C. Precipitates were dissolved in DMSO, and plates were analyzed on a Thermo MULTISKAN EX plate reader at 595 nm to determine IC_{50}; IC_{50} is the concentration required to kill 50% of the cell population.

■ ASSOCIATED CONTENT

Supporting Information

The Supporting Information is available free of charge on the ACS Publications website at DOI: 10.1021/acsomega.8b00706.

Absorption spectra of THAQ recorded in the presence of Co(II); note on the interaction of THAQ with Co(II) leading to the calculation of stability constant of the complex in solution; absorption spectra of THAQ in aqueous solution and its Co(II) complex in DMSO; infrared spectrum of THAQ and Co(II)−THAQ; mass spectrum of Co(II)−THAQ; EPR spectrum of Co(II)−THAQ; TGA of Co(II)−THAQ; probable structure of the prepared Co(II) complex of THAQ; plots showing the interaction of the compounds with calf thymus DNA using UV−vis spectroscopy and fluorescence spectroscopy; and short description of Fenton reactions due to Fe(III) and Cu(II) complexes leading to the generation of $^{\bullet}OH$ and the lack of it for other transition-metal ions of the first transition series (PDF)
(MOL)

■ AUTHOR INFORMATION

Corresponding Author

*E-mail: dasrsv@yahoo.in, sdas@chemistry.jdvu.ac.in. Phone: +91 33 24572148, +91 33 8902087756. Fax: +91 33 24146223 (S.D.).

ORCID

Saurabh Das: 0000-0002-0455-8760

Present Addresses

[⊥]Harinavi Subhasini Girls' High School, Kolkata, India.
[#]Department of Biotechnology, Sun Pharmaceutical Industries Limited, Tandalja, Vadodara 390020.
[¶]Environmental Engineering Section, MECON Limited (A Govt. of INDIA Enterprise), Ranchi 834002.
[▽]Chief, Basic Research, Saroj Gupta Cancer Centre and Research Institute, Mahatma Gandhi Road, Thakurpukur, Kolkata 700 063.

Notes

The authors declare no competing financial interest.

DOI: 10.1021/acsomega.8b00706
ACS Omega 2018, 3, 10255−10266

■ ACKNOWLEDGMENTS

This work was funded by the Department of Science &Technology, Govt. of West Bengal, India, in the form of an R & D project [794(Sanc.)1(10) ST/P/S&T/9G-23/2013] to S.D. S.D. is grateful to UGC, New Delhi, for funding the research program on Advanced Materials as part of UPE II to Jadavpur University from which funds were used for this work. He is also grateful to the DST-PURSE program of the Government of India for financial support to Jadavpur University and the DST-FIST program of the Government of India for providing the EPR facility to the Department of Chemistry, used in this work. He expresses his gratitude to Prof. Kalyan K. Mukherjea and his research scholars for help in procuring the EPR data. S.M.C. wishes to thank Dr. Durba Ganguly for her help in preparing some of the figures. Dr. Sanjay Kumar (Dept. of Physics, J U) and Dr. Shouvik Chattopadhyay (Dept. of Chemistry, J U) are appreciated for some useful discussions regarding the structure of the complex.

■ ABBREVIATIONS

THAQ, quinalizarin or 1,2,5,8-tetrahydroxy-9,10-anthraquinone; $Co^{II}(THAQ)_2$, Co^{II} complex of quinalizarin; quinalizarin, THAQ = QH_4; ROS, reactive oxygen species; SOD, superoxide dismutase; ETO, etoposide; CPT, camptothecin; DOX, doxorubicin

■ REFERENCES

(1) Arcamone, F.; Penco, S. Synthesis of new doxorubicin analogs. In *Anthracycline and Anthracenedione-Based Anticancer Agents*; Lown, J. W., Ed.; Elsevier: Amsterdam, The Netherlands, 1988; pp 1−53.

(2) Arcamone, F.; Cassinelli, G.; Fantini, G.; Grein, A.; Orezzi, P.; Pol, C.; Spalla, C. Adriamycin, 14-Hydroxydaunomycin, a new antitumor antibiotic from S. peucetius var.caesius. *Biotechnol. Bioeng.* **2000**, *67*, 704−713.

(3) Rubin, E. H.; Hait, W. N. Anthracyclines and DNA Intercalators/Epipodophyllotoxins/DNA topoisomerases. In *Holland-Frei Cancer Medicine*, 5th ed.; Bast, R. C., Jr., Kufe, D. W., Pollock, R. E., Weichselbaum, R. R., Holland, J. F., Eds.; B C Decker: Hamilton, 2000; Chapter 49.

(4) Wang, J. C. Cellular roles of DNA topoisomerases: a molecular perspective. *Mol. Cell. Biol.* **2002**, *3*, 430−440.

(5) Koster, D. A.; Crut, A.; Shuman, S.; Bjornsti, M.-A.; Dekker, N. H. Cellular strategies for regulating DNA supercoiling: a single-molecule perspective. *Cell* **2012**, *142*, 519−530.

(6) Pommier, Y. DNA Topoisomerase I inhibitors: Chemistry, biology, and interfacial inhibition. *Chem. Rev.* **2009**, *109*, 2894−2902.

(7) Pommier, Y. Camptothecins and Topoisomerase I; A Foot in the Door. Targeting the Genome Beyond Topoisomerase I with Camptothecins and Novel Anticancer Drugs; Importance of DNA Replication, Repair and Cell Cycle Checkpoints. *Curr. Med. Chem.: Anti-Cancer Agents* **2004**, *4*, 429−434.

(8) Pommier, Y.; Leo, E.; Zhang, H.; Marchand, C. DNA Topoisomerases and their poisoning by anticancer and antibacterial drugs. *Chem. Biol.* **2010**, *17*, 421−433.

(9) Pommier, Y. Topoisomerase I inhibitors: camptothecins and beyond. *Cancer* **2006**, *6*, 789−802.

(10) Das, P.; Jain, C. K.; Dey, S. K.; Saha, R.; Chowdhury, A. D.; Roychoudhury, S.; Kumar, S.; Majumder, H. K.; Das, S. Synthesis, crystal structure, DNA interaction and in vitro anticancer activity of a Cu(II) complex of purpurin: dual poison for human DNA topoisomerase I and II. *RSC Adv.* **2014**, *4*, 59344−59357.

(11) Banerjee, T.; Mukhopadhyay, R. Structural effects of nogalamycin, an antibiotic antitumour agent, on DNA. *Biochem. Biophys. Res. Commun.* **2008**, *374*, 264−268.

(12) Lipshultz, S. E.; Alvarez, J. A.; Scully, R. E. Anthracycline associated cardiotoxicity in survivors of childhood cancer. *Heart* **2008**, *4*, 525−533.

(13) Lenglet, G.; David-Cordonnier, M.-H. DNA-destabilizing agents as an alternative approach for targeting DNA: Mechanisms of action and cellular consequences. *J. Nucleic Acids* **2010**, 290935.

(14) Butler, J.; Hoey, B. M.; Swallow, A. J. Reactions of the semiquinone free radicals of anti-tumour agents with oxygen and iron complexes. *FEBS Lett.* **1985**, *182*, 95−98.

(15) Land, E. J.; Mukherjee, T.; Swallow, A. J.; Bruce, J. M. Possible intermediates in the action of adriamycin-a pulse radiolysis study. *Br. J. Cancer* **1985**, *51*, 515−523.

(16) Santra, R. C.; Ganguly, D.; Singh, J.; Mukhopadhyay, K.; Das, S. A study on the formation of the nitro radical anion by ornidazole and its significant decrease in a structurally characterized binuclear Cu(II)-complex: impact in biology. *Dalton Trans.* **2015**, *44*, 1992−2000.

(17) Santra, R. C.; Ganguly, D.; Jana, S.; Banyal, N.; Singh, J.; Saha, A.; Chattopadhyay, S.; Mukhopadhyay, K.; Das, S. Synthesizing a CuII complex of tinidazole to tune the generation of the nitro radical anion in order to strike a balance between efficacy and toxic side effects. *New J. Chem.* **2017**, *41*, 4879−4886.

(18) Avendano, C.; Menendez, J. C. *Medicinal Chemistry of Anticancer Drugs*, 1st ed.; Elsevier: Amsterdam, 2008.

(19) Fiallo, M. M. L.; Garnier-Suillerot, A. Physicochemical studies of the iron(III)-carminomycin complex and evidence of the lack of stimulated superoxide production by NADH deydrogenase. *Biochim. Biophys. Acta* **1985**, *840*, 91−98.

(20) Monti, E.; Paracchini, L.; Piccinini, F.; Malatesta, V.; Morazzoni, F.; Supino, R. Cardiotoxicity and antitumor activity of a copper(II)-doxorubicin chelate. *Cancer Chemother. Pharmacol.* **1990**, *25*, 333−336.

(21) Brahmachari, G. Natural products in drug discovery: Impacts and opportunities - An assessment. In *Bioactive Natural Products: Opportunities and Challenges in Medicinal Chemistry*; Brahmachari, G., Ed.; World Scientific Publishing: Singapore, 2012; pp 1−200.

(22) Das, P.; Guin, P. S.; Mandal, P. C.; Paul, M.; Paul, S.; Das, S. Cyclic voltammetric studies of 1, 2, 4-trihydroxy-9, 10-anthraquinone, its interaction with calf thymus DNA and anti-leukemic activity on MOLT-4 cell lines: A comparison with anthracycline anticancer drugs. *J. Phys. Org. Chem.* **2011**, *24*, 774−785.

(23) Braun, M.; Jacobs, V. R.; Wagenpfeil, S.; Sattler, D.; Harbeck, N.; Nitz, U.; Bernard, R.; Kuhn, W.; Ihbe-Heffinger, A. Cost analysis comparing an anthracycline/docetaxel regimen to CMF in patients with early stage breast cancer. *Onkologie* **2009**, *32*, 473−481.

(24) Das, S.; Saha, A.; Mandal, P. C. Studies on the formation of Cu(II) and Ni(II) complexes of 1,2-dihydroxy-9,10-anthraquinone and lack of stimulated superoxide formation by the complexes. *Talanta* **1990**, *43*, 95−102.

(25) Guin, P. S.; Das, S.; Mandal, P. C. Studies on the formation of a complex of Cu(II) with sodium 1,4-dihydroxy-9,10-anthraquinone-2-sulphonate - An analogue of the core unit of anthracycline anticancer drugs and its interaction with calf thymus DNA. *J. Inorg. Biochem.* **2009**, *103*, 1702−1710.

(26) Guin, P. S.; Mandal, P. C.; Das, S. The Binding of a Hydroxy-9,10-anthraquinone CuII Complex to Calf Thymus DNA: Electrochemistry and UV/Vis Spectroscopy. *ChemPlusChem* **2012**, *77*, 361−369.

(27) Guin, P. S.; Mandal, P. C.; Das, S. A comparative study on the interaction with calf thymus DNA of a Ni(II) complex of the anticancer drug adriamycin and a Ni(II) complex of sodium 1,4-dihydroxy-9,10-anthraquinone-2-sulphonate. *J. Coord. Chem.* **2012**, *65*, 705−721.

(28) Tevyashova, A. N.; Klyosov, A. A.; Olsufyeva, E. N.; Preobrazhenskaya, M. N.; Zomer, E. Synthesis and Biological Activity of Galactomycin and DoxoDavanat, New Conjugates of Doxorubicin with D-Galactose and 1,4-β-D-Galactomannan. *ACS Symp. Ser.*, Glycobiology and Drug Design, 2012; Vol. *1102*, Chapter 5, pp 131−154.

DOI: 10.1021/acsomega.8b00706
ACS Omega 2018, 3, 10255−10266

(29) Mukherjee, S.; Das, P.; Das, S. Exploration of small hydroxy-9,10-anthraquinones as anthracycline analogues: physicochemical characteristics and DNA binding for comparison. *J. Phys. Org. Chem.* **2012**, *25*, 385−393.
(30) Verebová, V.; Adamcik, J.; Danko, P.; Podhradský, D.; Miškovský, P.; Staničová, J. Anthraquinones quinizarin and danthron unwind negatively supercoiled DNA and lengthen linear DNA. *Biochem. Biophys. Res. Commun.* **2014**, *444*, 50−55.
(31) Mukherjee, S.; Gopal, P.; Paul, S.; Das, S. Acetylation of 1,2,5,8-tetrahydroxy-9,10- anthraquinone improves binding to DNA and showed enhanced superoxide formation that explains better cytotoxicity on Jurkat T lymphocyte cells. *J. Anal. Oncol.* **2014**, *3*, 122−129.
(32) Cozza, G.; Mazzorana, M.; Papinutto, E.; Bain, J.; Elliott, M.; di Maira, G.; Gianoncelli, A.; Pagano, M. A.; Sarno, S.; Ruzzene, M.; Battistutta, R.; Meggio, F.; Moro, S.; Zagotto, G.; Pinna, L. A. Quinalizarin as a potent, selective and cell-permeable inhibitor of protein kinase CK2. *Biochem. J.* **2009**, *421*, 387−395.
(33) Zhou, Y.; Li, K.; Zhang, S.; Li, Q.; Li, Z.; Zhou, F.; Dong, X.; Liu, L.; Wu, G.; Meng, R. Quinalizarin, a specific CK2 inhibitor, reduces cell viability and suppresses migration and accelerates apoptosis in different human lung cancer cell lines. *Ind. J. Cancer.* **2015**, *52*, e119−e123.
(34) Litchfield, D. W. Protein kinase CK2: structure, regulation and role in cellular decisions of life and death. *Biochem. J.* **2003**, *369*, 1−15.
(35) Jabłońska-Trypuć, A.; Swiderski, G.; Krętowski, R.; Lewandowski, W. Newly synthesized doxorubicin complexes with selected metals—Synthesis, structure and anti-breast cancer activity. *Molecules* **2017**, *22*, 1106.
(36) Nakamoto, K. *Infrared and Raman Spectra of Inorganic and Coordination Compounds*, 3rd ed.; Wiley-Interscience: New York, 1978.
(37) Baumgarten, M.; Winscom, C. J.; Lubitz, W. Probing the surrounding of a cobalt(II) porphyrin and its superoxo complex by EPR techniques. *Appl. Magn. Reson.* **2001**, *20*, 35−70.
(38) Tachibana, M.; Iwaizumi, M. EPR studies of copper(II) and cobalt(II) complexes of adriamycin. *J. Inorg. Biochem.* **1987**, *30*, 133−140.
(39) Tachibana, M.; Iwaizumi, M. EPR and UV-visible spectroscopic studies of copper(II) and cobalt(II) complexes of hydroxyanthraquinones. *J. Inorg. Biochem.* **1987**, *30*, 141−151.
(40) Di Vaira, M.; Orioli, P.; Piccioli, F.; Bruni, B.; Messori, L. Structure of a Terbium(III)−Quinizarine Complex: The First Crystallographic Model for Metalloanthracyclines. *Inorg. Chem.* **2003**, *42*, 3157−3159.
(41) Mandal, B.; Singha, S.; Dey, S. K.; Mazumdar, S.; Mondal, T. K.; Karmakar, P.; Kumar, S.; Das, S. Synthesis, crystal structure from PXRD of a MnII(purp)2 complex, interaction with DNA at different temperatures and pH and lack of stimulated ROS formation by the complex. *RSC Adv.* **2016**, *6*, 51520−51532.
(42) Mandal, B.; Singha, S.; Dey, S. K.; Mazumdar, S.; Kumar, S.; Karmakar, P.; Das, S. CuII complex of emodin with improved anticancer activity as demonstrated by its performance on HeLa and Hep G2 cells. *RSC Adv.* **2017**, *7*, 41403−41418.
(43) Zarembowitch, J.; Kahn, O. Magnetic properties of some spin-crossover, high-spin, and low-spin cobalt(II) complexes with Schiff bases derived from 3-formylsalicylic acid. *Inorg. Chem.* **1984**, *23*, 589−593.
(44) Frisch, M. J.; Trucks, G. W.; Schlegel, H. B.; Scuseria, G. E.; Robb, M. A.; Cheeseman, J. R.; Scalmani, G.; Barone, V.; Petersson, G. A.; Nakatsuji, H.; Li, X.; Caricato, M.; Marenich, A. V.; Bloino, J.; Janesko, B. G.; Gomperts, R.; Mennucci, B.; Hratchian, H. P.; Ortiz, J. V.; Izmaylov, A. F.; Sonnenberg, J. L.; Williams-Young, D.; Ding, F.; Lipparini, F.; Egidi, F.; Goings, J.; Peng, B.; Petrone, A.; Henderson, T.; Ranasinghe, D.; Zakrzewski, V. G.; Gao, J.; Rega, N.; Zheng, G.; Liang, W.; Hada, M.; Ehara, M.; Toyota, K.; Fukuda, R.; Hasegawa, J.; Ishida, M.; Nakajima, T.; Honda, Y.; Kitao, O.; Nakai, H.; Vreven, T.; Throssell, K.; Montgomery, J. A., Jr.; Peralta, J. E.; Ogliaro, F.; Bearpark, M. J.; Heyd, J. J.; Brothers, E. N.; Kudin, K. N.; Staroverov, V. N.; Keith, T. A.; Kobayashi, R.; Normand, J.; Raghavachari, K.; Rendell, A. P.; Burant, J. C.; Iyengar, S. S.; Tomasi, J.; Cossi, M.; Millam, J. M.; Klene, M.; Adamo, C.; Cammi, R.; Ochterski, J. W.; Martin, R. L.; Morokuma, K.; Farkas, O.; Foresman, J. B.; Fox, D. J. *Gaussian 09*, Revision A.02; Gaussian, Inc.: Wallingford CT, 2016.
(45) Scatchard, G. The attractions of proteins for small molecules and ions. *Ann. N.Y. Acad. Sci.* **1949**, *51*, 660−672.
(46) Noh, S. M. Measurement of peritoneal fluid pH in patients with non-serosal invasive gastric cancer. *Yonsei Med. J.* **2003**, *44*, 45−48.
(47) Huang, C.-H.; Mong, S.; Crooke, S. T. Interactions of a new antitumor antibiotic BBM-928A with deoxyribonucleic acid. Bifunctional intercalative binding studied by fluorometry and viscometry. *Biochemistry* **1980**, *19*, 5537−5542.
(48) Mahler, H. R. *Methods in Enzymology* 11; Colowick, S. P., Kaplan, N. O., Eds.; Academic Press: New York, USA, 1955; pp 668−672.
(49) Koppenol, W. H.; Van Buuren, K. J. H.; Butler, J.; Braams, R. The kinetics of the reduction of cytochrome *c* by the superoxide anion radical. *Biochim. Biophys. Acta* **1976**, *449*, 157−168.
(50) Fiallo, M. M. L.; Garnier-Suillerot, A. Metal anthracycline complexes as a new class of anthracycline derivatives. *Inorg. Chim. Acta* **1987**, *137*, 119−121.
(51) Das, S.; Bhattacharya, A.; Mandal, P. C.; Rath, M. C.; Mukherjee, T. One-electron reduction of 1,2-dihydroxy-9,10-anthraquinone and some of its transition metal complexes in aqueous solution and in aqueous isopropanol-acetone-mixed solvent: A steady-state and pulse radiolysis study. *Rad. Phys. Chem.* **2002**, *65*, 93−100.
(52) Gammella, E.; Maccarinelli, F.; Buratti, P.; Recalcati, S.; Cairo, G. The role of iron in anthracycline cardiotoxicity. *Front. Pharmacol.* **2014**, *5*, 1−6.
(53) Liochev, S. I.; Fridovich, I. Superoxide and Iron: Partners in Crime. *IUBMB Life* **1999**, *48*, 157−161.
(54) Roy, S.; Mondal, P.; Sengupta, P. S.; Dhak, D.; Santra, R. C.; Das, S.; Guin, P. S. Spectroscopic, computational and electrochemical studies on the formation of the copper complex of 1-amino-4-hydroxy-9,10-anthraquinone and effect of it on superoxide formation by NADH dehydrogenase. *Dalton Trans.* **2015**, *44*, 5428−5440.
(55) Lipinski, B. Hydroxyl radical and its scavengers in health and disease. *Oxid. Med. Cell. Longevity*, **2011**, *2011*, Article ID 809696, 9 pages.
(56) Das, S.; Saha, A.; Mandal, P. C. Radiation-Induced Double-Strand Modification in Calf Thymus DNA in the Presence of 1,2-Dihydroxy-9,10-Anthraquinone and Its Cu(II) Complex. *Environ. Health Perspect.* **1997**, *105*, 1459−1462.
(57) Fiallo, M. M. L.; Garnier-Suillerot, A.; Matzanke, B.; Kozlowski, H. How Fe3+ binds anthracycline antitumour compounds. *J. Inorg. Biochem.* **1999**, *75*, 105−115.
(58) Buontempo, F.; Orsini, E.; Martins, L. R.; Antunes, I.; Lonetti, A.; Chiarini, F.; Tabellini, G.; Evangelisti, C.; Evangelisti, C.; Melchionda, F.; Pession, A.; Bertaina, A.; Locatelli, F.; McCubrey, J. A.; Cappellini, A.; Barata, J. T.; Martelli, A. M. Cytotoxic activity of the casein kinase 2 inhibitor CX-4945 against T-cell acute lymphoblastic leukemia: targeting the unfolded protein response signaling. *Leukemia* **2014**, *28*, 543−553.
(59) Boyer, J.; McLean, E. G.; Aroori, S.; Wilson, P.; McCulla, A.; Carey, P. D.; Longley, D. B.; Johnston, P. G. Characterization of p53 wild-type and null isogenic colorectal cancer cell lines resistant to 5-fluorouracil, oxaliplatin, and irinotecan. *Clin. Cancer Res.* **2004**, *10*, 2158−2167.
(60) Shin, D. H.; Choi, Y.-J.; Park, J.-W. SIRT1 and AMPK mediate hypoxia-induced resistance of non-small cell lung cancers to cisplatin and doxorubicin. *Cancer Res.* **2014**, *74*, 298−308.
(61) Dabholkar, M.; Parker, R.; Reed, E. Determinants of cisplatin sensitivity in non-malignant non-drug-selected human T cell lines. *DNA Repair* **1992**, *274*, 45−56.
(62) Antunovic, M.; Kriznik, B.; Ulukaya, E.; Yilmaz, V. T.; Mihalic, K. C.; Madunic, J.; Marijanovic, I. Cytotoxic activity of novel

DOI: 10.1021/acsomega.8b00706
ACS Omega 2018, 3, 10255−10266

palladium-based compounds on leukemia cell lines. *Anti-Cancer Drugs* **2015**, *26*, 180−186.

DOI: 10.1021/acsomega.8b00706
ACS Omega 2018, 3, 10255−10266